©KY PUBLICATIONS
**International Journal of Chemistry and Aquatic Sciences (IJCA)**
**Vol.10.Issue.4.2024(Oct-Dec) Page 1-14**
**ISSN: 2355-033X**
**Research Article**

# Synthesis of Mn-Zn-$Fe_2O_4$ nanoparticle composites with reduced graphene oxide (rGO) for potential application in spintronics and optoelectronics

**Dr Moustfa M.H. Eshtewi[1], Dr. Hamed Mohamed Abubaker Malek[2]**
[1]*Libyan Authority for Scientific Research*
[2]*Department of Physics Faculty of Science, Sebha University, Libya.*

doi: 10.33329/ijca.10.4.1


**Article info**
Article Received:19/10/2024
Article Accepted: 11/11/2024
Published online:23/12/2024

**ABSTRACT**

In this study, $Mn_{0.7}Zn_{0.3}Fe_2O_4$ nanoparticles were synthesized using the sol-gel auto-combustion method, while reduced graphene oxide (rGO) was prepared by the modified Hummers method. The rGO/$Mn_{0.7}Zn_{0.3}Fe_2O_4$ nanocomposites were synthesized through ultrasound-assisted dispersion. The structural and phase properties of the composites were analyzed using X-ray Powder Diffraction (XRD), confirming the formation of a spinel structure with rhombohedral symmetry. The average particle size of $Mn_{0.7}Zn_{0.3}Fe_2O_4$ was found to be 9.8 nm, with a Gaussian particle size distribution ranging from 4 to 10 nm. UV-Vis spectroscopy revealed the optical characteristics of rGO, while the magnetic properties, assessed via a vibrating sample magnetometer, indicated that the composite retained the magnetic behavior typical of ferrites. The composite exhibited a band gap (Eg) of 1.09 eV, lower than that of pure $Mn_{0.7}Zn_{0.3}Fe_2O_4$ (1.4 eV), suggesting the formation of new energy levels due to the presence of rGO. Energy Dispersive X-ray Spectroscopy (EDS) analysis of the rGO/$Mn_{0.7}Zn_{0.3}Fe_2O_4$ nanocomposite showed a composition of 71.4% carbon, 20.3% oxygen, 5.7% iron, 1.6% manganese, and 0.9% zinc. The materials exhibited semiconductor behavior, with Eg values confirming their potential as photocatalysts. Magnetization curves showed that the composite ferrite behaved as a soft ferromagnetic material, with a saturation magnetization of 37.04 emu/g. The composite's reduced band gap, coupled with its magnetic and photocatalytic properties, makes it a promising candidate for spintronic and optoelectronic applications, as well as a catalyst in photo-Fenton processes.
Keywords: $Mn_{0.7}Zn_{0.3}Fe_2O_4$, reduced graphene oxide (rGO), nanocomposites, Characterization, band gap (Eg), magnetic properties.

## Introduction

The rapid advancement of nanomaterials has opened new avenues for the development of functional devices with novel properties and applications. Among various types of nanoparticles, ferrite-based nanocomposites, such as Mn-Zn-$Fe_2O_4$, have attracted significant attention due to their unique magnetic, electrical, and optical properties. These ferrite nanoparticles are particularly promising for applications in spintronics, optoelectronics, and energy storage. The combination of these ferrites with reduced graphene oxide (rGO), a material known for its excellent electrical conductivity,

high surface area, and mechanical strength, has the potential to enhance the performance and functionality of these composites, making them highly suitable for advanced applications in modern electronics.

Spinels have been substituted for manganese by zinc and have great potential in various applications, highlighting their relevance in the field of spintronics and optoelectronics. $Mn-Zn-Fe_2O_4$ nanoparticles have attracted attention in various areas of research due to their characteristics, such as their superparamagnetic nature, optical properties, and their Curie temperature [1]. In addition, the scientific literature [1-2] has pointed out that the graphene family is highly compatible with other compounds and has applications in the field of spintronics, and optoelectronics, among others. Reduced graphene oxide (GO), which combines properties of graphene and graphene oxide, stands out for its hydrophilicity, which gives it high solubility in water and facilitates its functionalization with other materials [3]. Recent research [4] has demonstrated improvements in properties such as colloidal stability and specific absorption by creating composites of magnetic materials with components of the graphene family. Therefore, research has been carried out on composites of GO with other materials to improve already known properties or develop new applications in different research fields [5].

It is known that $MnFe_2O_4$ /GO composites can be obtained by solvothermal method using chlorides as precursors in the case of spinel, and for the composite they used a modification to the Hummers method to achieve the decoration in reduced graphene oxide, obtaining good results compared to combustion and microwave methods, achieving smaller particle size and low particle agglomeration [6]. For this reason, it has been decided to use the solvothermal method to synthesize the nanoparticles with their different proposed concentrations. The method is considered to be of mild chemistry since it is in a closed environment and does not need much energy, therefore, there will be less environmental impact. On the other hand, the substitution of Zinc by Manganese is proposed to modify its band gap in the visible range and the magnetization. These elaborated investigations show us that it is feasible and interesting to synthesize, characterize and study the proposed composites [7].

Magnetic composites are highly valued for their versatility in electromagnetic applications. Magnetic nanoparticles are preferred because of their magnetic properties, which include superparamagnetism [8], high coercivity, a low Curie temperature, and increased magnetic sensitivity. Several types of iron oxides have been extensively studied over the last decade. Researchers from various disciplines are very interested in magnetic nanoparticles. For this purpose, publications of some research on these compounds that have been analyzed for their possible application in multidisciplinary fields were analysed [9].

Abdel-Fattah Omran et al. (2014) [10] synthesised $Zn_{0.2}Mn_{0.8}Fe_2O_4$ ferrite nanoparticles coated with polyaniline, creating a composite structure via sol-gel combustion, with composite samples characterised by XRD, FT-IR, TEM, TGA, and VSM measurements. XRD, FTIR, and UV-vis spectral analyses validated the synthesis of ZnMn ferrite composites with an average particle size of 45 nm. The nanocomposites exhibited hysteresis loops indicative of superparamagnetic behaviour ($10^4$ emu/g) when subjected to an applied magnetic field at room temperature. Othman et al. [11] synthesised $M_xMn_{1-x}Fe_2O_4$ spinel ferrites (M=Zn or Cd; x=0.0 or 0.2) using the coprecipitation method. The optical band gap decreased from 2.8 eV for $Zn_{0.2}Mn_{0.8}Fe_2O_4$ and $MnFe_2O_4$. These findings suggest that this type of magnetic adsorbent is both viable and cost-effective for wastewater treatment. This paper does not include a magnetisation test. Anwar et al. [12] synthesised $ZnFe_2O_4$ using nitrate precursors and a fuel-assisted microwave combustion method. Rietveld analysis and Fourier transform infrared (FT-IR) determined the average size to be within the favourable range of 37.57 nm to 25.43 nm. Energy dispersive X-ray (EDX) analysis verified the elemental composition and purity of the samples. Arguello Cruz,(2023) [13] illustrated exchange coupling in core-shell magnetic nanostructures, wherein the core and shell constituents consist of magnetic ferrites ($Fe_3O_4$, $MnFe_2O_4$ and $Zn_{0.2}Mn_{0.8}Fe_2O_4$) synthesised

via the solvothermal method utilising acetyl acetates as precursors. The particle size was assessed using TEM, yielding an average size between 8 and 15 nm. Due to their biocompatibility and superior therapeutic properties, the exchange-coupled core-shell nanoparticles exhibit significant potential in diagnostic imaging and drug delivery applications. Novel magnetic nanomaterials comprising graphene oxide and MgO-$MgFe_2O_4$ were synthesised by Medina, et al. (2020) [14] through a hydrothermal method utilising magnesium and iron nitrates. The molar ratio of Fe to Mg was 1:1, and it was observed that the GO-based nanocomposite exhibited magnetic properties by forming a new $MgFe_2O_4$ phase rather than the α-$Fe_2O_3$ phase, as confirmed by XRD analysis. FE-SEM and HRTEM analyses validated the synthesis of a MgO-$MgFe_2O_4$ nanocomposite on the GO substrate, exhibiting a diameter of approximately 30-80nm. The study demonstrated that the GO-based nanocomposite is an innovative, highly effective material that can be repeatedly utilised, as it can be retrieved via a magnetic field, making it particularly advantageous for addressing decontamination issues.

Spintronics, which exploits the intrinsic spin of electrons, and optoelectronics, which involves the interaction of light with electronic materials, are two rapidly growing fields that benefit from the development of multifunctional nanomaterials. The integration of magnetic nanoparticles like Mn-Zn-$Fe_2O_4$ with rGO can enable improved charge transport, spin manipulation, and light-matter interaction, thus broadening their scope for use in sensors, memory devices, photovoltaic cells, and light-emitting diodes (LEDs).

Although significant progress has been made in the synthesis of metal ferrite-based nanocomposites, the development of Mn-Zn-$Fe_2O_4$-rGO nanocomposites for spintronic and optoelectronic applications is still an emerging area with substantial gaps in knowledge. Several studies have focused on the individual properties of Mn-Zn-Fe2O4 and rGO, but comprehensive research exploring their synergistic interactions and how these interactions enhance device performance is limited. The synthesis routes, structural characteristics, and fundamental understanding of the material properties at the nanoscale, including the role of graphene oxide in improving the magnetic and optoelectronic behavior of ferrites, are under-explored. Moreover, the precise control of nanoparticle size, morphology, and the degree of graphene reduction is crucial for optimizing the composite properties, yet it remains a challenge.

The primary objective of this study is to synthesize Mn-Zn-Fe2O nanoparticles and form nanocomposites with reduced graphene oxide (rGO) to investigate their potential applications in spintronics and optoelectronics. Specifically, the study aims to synthesize rGO/$Mn_{0.7}$-$Zn_{0.3}Fe_2O_4$ **Characterize the structural, magnetic, and optical properties** and **explore the influence of Zn-Mn-Fe2O4-rGO composites** using controlled methods to achieve uniform dispersion and optimized interactions between the ferrite nanoparticles and graphene oxide. By addressing these objectives, the study will contribute to advancing the design of multifunctional nanocomposites that can meet the demands of next-generation spintronic and optoelectronic devices.

## 2. Materials and Methods

### 2.1 Materials

Thermo Scientific Furnace, ice container, measuring flask, volume pipette, dropper, magnetic stirrer, measuring cylinder, beaker, Erlenmeyer flask, spray bottle, funnel, Whatman 41 filter paper, analytical balance Galaxy 160 Ohaus, porcelain cup, Teflon and stainless-steel container, ultrasonic cleaner Krisbow, Health H-C-8 centrifuge, graphite powder (Merck), Zn powder (Merck), and distilled water and other reagents obtained from Merck, SD fine chemicals with 98% purity AR grade chemicals.

**Sol-gel auto combustion synthesis for obtaining $Mn_{0.7}Zn_{0.3}Fe_2O_4$**

The samples were prepared by the sol-gel auto combustion method using two different fuels (glycine and urea) and a surfactant cetyltrimethylammonium bromide (CTAB). For the synthesis, the precursor metal salts, as well as the fuels, glycine and urea, and the surfactant hexadecyltrimethylammonium bromide, were used of a purity grade ≥ 97% and obtained from Sigma Aldrich. The reagents were weighed in stoichiometric quantities with a ratio of 1:0.8:0.1 of salts to fuel to surfactant respectively, then they were added to 100 ml of distilled water in a beaker to obtain a solution. Then, it was placed on a thermal plate to be subjected to magnetic stirring and continuous heating until the solution reached a temperature of 100 °C leading to the formation of a gel, which caused a change in color from reddish to a very dark brown almost black. Subsequently, the gel was placed in an alumina crucible and introduced into a muffle furnace to carry out a heating at 600 °C for 1 hour to produce the auto-combustion of the gel. Next, the ferrite powders were obtained, which were ground in an agate mortar and placed in vials for their respective characterizations.

**Synthesis of reduced graphene oxide (rGO) by the modified Hummers method [15]**: The synthesis of rGO was carried out by the modified Hummers method, in which graphite oxide is first obtained and then exfoliation is carried out to produce graphene oxide, and finally reduction is carried out to obtain reduced graphene oxide. The precursors used were graphite powder, concentrated sulfuric acid, sodium nitrate, potassium permanganate, hydrogen peroxide and hydrochloric acid, all reagents with a purity of 98%. For its preparation, beakers, an agate mortar, a heating plate with magnetic stirring, a magnetic stirrer, a centrifuge, an ultrasonic bath and a muffle with controlled heating were used.

**From graphite powder to graphite oxide:** In a beaker, add 25 ml of concentrated sulfuric acid and 0.5 g of graphite, stirring constantly at room temperature (just to mix the acid with the graphite). Next, add 0.5 g of sodium nitrate and place the beaker with the mixture in an ice bath to lower the temperature of the mixture to approximately 5 °C. This is achieved faster with the help of acetone and salt in the ice. Then, add 3 g of potassium permanganate little by little very carefully, since it is a strong oxidant and can cause an explosion if not kept at a low temperature. Then, put it in a water bath so that the solution rises to 40 °C, reaching it, leave it for 30 min stirring and at a constant temperature. The next step is to add 50 ml of distilled water and again increase the temperature of the solution to 90 °C and leave it under magnetic stirring at a constant temperature for 15 min. After this time, 150 ml of distilled water are added to the solution, followed by a slow addition of 10 ml of hydrogen peroxide and it is observed that it changes from a brown color to a yellow one. Subsequently, 90 ml of 4% HCl are added and approximately 11 washes with distilled water are carried out until reaching a pH value in the range of 6 to 7, using centrifugation. Next, it is incorporated into the muffle for drying at 100 °C for 24 hours. Finally, it is removed from the muffle, the powder reaches room temperature and is ground in the agate mortar.

**Exfoliation of graphite oxide and obtaining graphene oxide (GO):** After obtaining the oxidation of graphite, its exfoliation was carried out as follows: 0.25 g of graphite oxide powder was weighed and added to 250 ml of distilled water in a beaker. An ultrasound bath was used to homogenize the solution for one hour. Afterwards, drying was carried out in a muffle at 100 °C for 24 hours. Next, the powders obtained were ground in the mortar for approximately 15 minutes. Then, the samples were sent to be characterized by different techniques.

**Chemical reduction of GO:** 0.25 g of GO is weighed and added to a beaker with 250 ml of distilled water. Then, 0.09 g of ascorbic acid is added and the beaker is placed on a hotplate for magnetic stirring for 15 minutes. The solution is then introduced into a controlled heating muffle at a temperature of 100 °C for 24 hours, during which time it is dried. Afterwards, the rGO powders obtained are ground in an

agate mortar for approximately 15 minutes to place the samples in vials and send them to be characterized by the required techniques.

**Synthesis of rGO/$Mn_{0.7}$-$Zn_{0.3}Fe_2O_4$ nanocomposites by ultrasound**: To obtain rGO/ferrite nanocomposites, $Mn_{0.7}$-$Zn_{0.3}Fe_2O_4$ ferrites and rGO are weighed in stoichiometric quantities with respect to the 1:0.97 ratio of ferrite to rGO, and then the compounds are added to a beaker with 250 ml of distilled water. Then, they are added to an ultrasound bath for particle dispersion, which was carried out for a time of 1 hour. Next, the solution is placed on a heating plate with magnetic stirring for 1 hour at 60 °C. The material is then introduced into a controlled heating muffle at a temperature of 100 °C for 24 hours for drying. Finally, the powder of rGO/$Mn_{0.7}Zn_{0.3}Fe_2O_4$ is obtained and sent to the corresponding characterization techniques.

**Characterization Studies**

In the characterization studies of the synthesized composite material; crystal structures and the phases contained therein were determined with an X-ray Powder Diffraction (XRD) device (X-ray Brucker D2 Phaser with wavelength (Cu 1.5418 Å), the intensity was measured in the 2θ range from 5$^o$ to 90$^o$ with a step size of 0.05° every 0.5s), functional groups were determined with Fourier Transform Infrared Spectroscopy (FT-IR) (Perkin Elmer Pragon1000PC brand spectrophotometer) device, surface morphology, particle and pore size was determined with Scanning Electron Microscopy (SEM-JEOL JSM6701F model)-Energy dispersive spectrophotometry (EDS-JEOL JSM6701F model), the UV-Vis technique was used to characterize reduced graphene oxide (rGO). The absorbance was measured at the wavelength of maximum adsorption of the specimen and to perform these measurements, a Shimadzu UV-Vis Spectrophotometer, model UV-18000, was used. The magnetic properties were determined in a vibrating sample magnetometer (LakeShore 7410) at room temperature and magnetic field of ± 15 kG.

**3. Results and Discussions**

It is essential to find the appropriate synthesis parameters to obtain a compound that has the desired crystalline structure, purity and crystallite size to carry out a scientific investigation and thus determine the impact it will have on the application(s) that could be considered. The synthesis of ferrites was successful with the solvothermal method, where the precursors used were acetylacetonates, compared to the theoretical framework, these use lower temperatures, and as described in the previous chapter, to obtain the spinel structure of the prepared ferrite rGO/$Mn_{0.7}$-$Zn_{0.3}Fe_2O_4$.

**XRD analysis:** The crystal structure of the ferrites was analysed by X-ray diffraction; the results revealed the formation of the spinel-type phase (Figure 1), similar to $MnFe_2O_4$ [16] and $ZnFe_2O_4$ [17], with a cubic structure and space group Fd-3m, indexed by the JCPDS file 74-2399. As mentioned, the XRD technique allows us to know these characteristics of our samples, therefore, in this project, the materials obtained were analysed by XRD. The XRD patterns of $Mn_{0.7}$-$Zn_{0.3}Fe_2O_4$ ferrites is shown in Figure 1. It was carried out in a 2θ diffraction range of 10° to 70° in which all the signals are shown well indexed in the (2-2-0), (3-1-1), (2-2-2), (4-0-0), (4-2-2), (5-1-1) and (4-0-0) planes respectively. The spinel $Mn_{0.7}$-$Zn_{0.3}Fe_2O_4$ was formed with a rhombohedral structure and space group R-3c indexed by the JCPDS file 72-469. No peaks related to the reflection of the crystal planes of the $MnO_2$, ZnO or $ZnO_2$ phases were identified. Thus, the presence of the α-$Fe_2O_3$ phase can be explained by the relative stability of the $Fe^{3+}$ cations in the tetrahedral sites (A), as well as by the influence of the atmosphere on the equilibrium involving oxygen gas and interstitial oxygen ions.

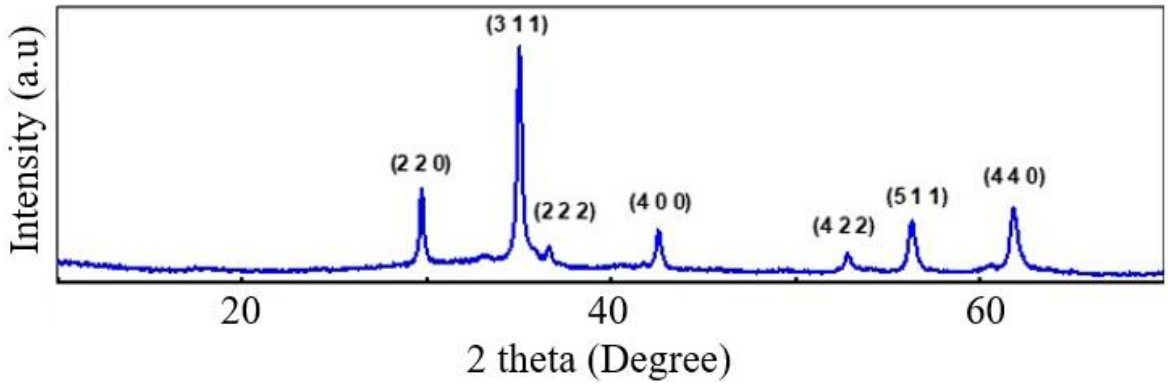


Figure 1: XRD patterns of the $Mn_{0.7}$-$Zn_{0.3}Fe_2O_4$ samples

The average crystallite size of each composition of $Mn_{0.7}$-$Zn_{0.3}Fe_2O_4$ ferrite was calculated from the Debye Scherrer equation [18], which is given by equation (1).

$$D = \frac{k\lambda}{\beta cos\theta} \quad (1)$$

where D is the crystallite size in nm, k is the constant (≈0.94), λ is the wavelength of X-ray radiation (0.15406 nm), β is the half-maximum full width of the signal and θ represents the diffraction angle.

The average crystallite size of the sample $Mn_{0.7}$-$Zn_{0.3}Fe_2O_4$ was 12.47 nm. The lattice parameter (a) and the unit cell volume (V) of the nanoparticle was determined from equations (2) and (3), respectively, based on the cubic structure of the spinel.

$$a = d\sqrt{h2 + k2 + l2} \quad (2)$$

$$V = a3 \quad (3)$$

where d is the interplanar distance that was determined with Bragg's Law (equation 4) and h, k and l are the indices of the system of planes also known as Miller indices.

$$d = \lambda / 2sin\theta \quad (4)$$

The values of the lattice parameters of $Mn_{0.7}$-$Zn_{0.3}Fe_2O_4$ is 4.9189 Å, and the unit cell volume is 119.0156 Å3. These results may be due to different factors, such as lattice defects, crystallite size [126].

Figure 2 shows the XRD patterns of the GO and rGO compounds, the interplanar distances were calculated with Bragg's law (equation 4) of the signal (0 0 1) in the case of GO and (0 0 2) of rGO, the values obtained were 7.55 Å and 3.68 Å, respectively, therefore, the value of the interplanar distance decreased when chemically reducing GO. This is explained by the existence of hydroxyl, epoxy and carbonyl functional groups in GO, consequently, when obtaining rGO these groups are reduced and thus the restoration of the $sp^2$ network is confirmed. Table 3 shows the interplanar distances of the GO and rGO compounds of this work in comparison with the research of Zhuangjun Fan et al [19]. Furthermore, the large difference in signal intensity at 2θ = 11.7° of the XRD pattern of GO compared to rGO is also indicative that the oxygen functional groups were reduced by a very considerable percentage [20].

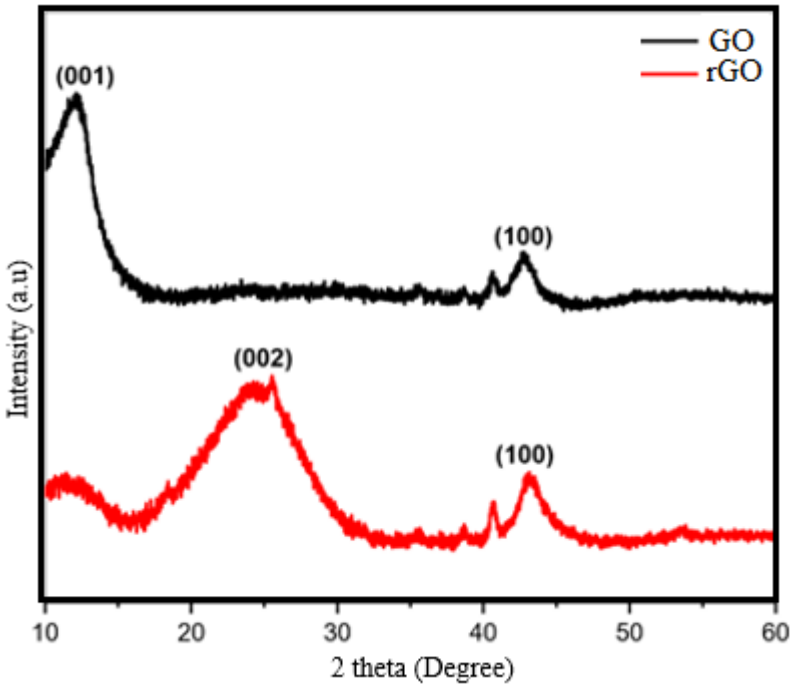


Figure 2. XRD patterns of samples GO and rGO

Our diffractogram is very similar to that of the literature by L. Stobinski et al [21] where the diffractograms of commercial GO and rGO with 99% purity are shown. In the case of GO the signal (1 0 0) was obtained at 2θ = 42.26°, whereas in our research it is at 2θ = 42.73°; Regarding the rGO of the literature, the signal (0 0 2) is found at 2θ = 23.76°, comparing with our work, we observe that signal at 2θ = 24.54°, the signal (1 0 0) of the rGO in the literature was obtained at 2θ = 42.74° and is very similar to our signal at 2θ = 43.06°, so we can verify that the desired compounds are obtained, the differences of a few tenths with the literature may be due to the synthesis method since they used commercial compounds.

The XRD patterns of the comparison of $Mn_{0.7}$-$Zn_{0.3}Fe_2O_4$ with its nanocomposite and rGO are shown in Figure 3. It is observed that the $Mn_{0.7}$-$Zn_{0.3}Fe_2O_4$ signals coincide with those of rGO/$Mn_{0.7}$-$Zn_{0.3}Fe_2O_4$, thus maintaining the cubic spinel structure, and it is also analysed that in the rGO/ferrite composite a slight addition of the (0 0 2) plane of rGO is seen, however, with a very low intensity and this confirms the grafting of the NPFE's on the rGO sheets. According Adeel Ahmed et al (2021) [22] our material signal from the (0-0-2) plane in the rGO/$Mn_{0.7}$-$Zn_{0.3}Fe_2O_4$ nanocomposite is observable, it is worth mentioning that the signal has very low intensity, so it could be said that the dispersion of the NPs in the rGO sheets is not completely homogeneous, but it is not so worrying due to the low intensity, then, most of the particles are well dispersed in the rGO sheets.

**FTIR analysis of GO and rGO compounds**

The FTIR spectra of GO and its reduction are shown in Figure 4, which reveal the presence of oxygen-containing functional groups in GO. The absorption band at 3324 cm-1 is a stretching of a hydroxyl group, the signal at 1724 cm-1 is due to a carbonyl group, the absorption at 1618 cm-1 is related to the stretching of the alkene group, an alkyl functional group is shown in the signal at 1377 cm-1, in the absorption at 1200 cm-1 we observe a carboxylic group and the signal at 1608 cm-1 belongs to an epoxide group. In our spectrum we observe that all the corresponding signals in rGO have lower intensities compared to GO, thus, the successful reduction is confirmed [23]. Table 4 shows a comparison of the absorption bands obtained in this work for the GO and those recorded in their

research by Ghann et al (2019) [24], where it can be seen that the values they showed are very similar to ours.

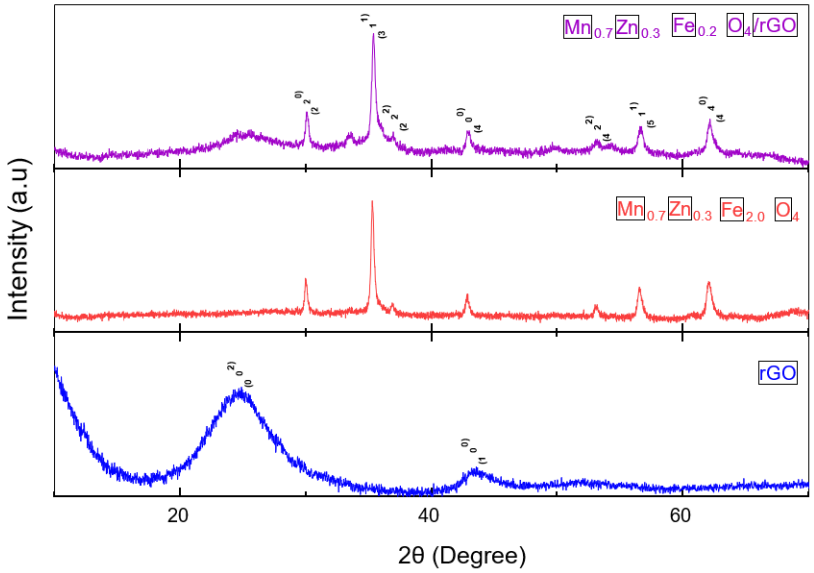


Figure 3. XRD pattern of the rGO/$Mn_{0.7}$-$Zn_{0.3}Fe_2O_4$, $Mn_{0.7}$-$Zn_{0.3}Fe_2O_4$ and rGO samples, respectively.

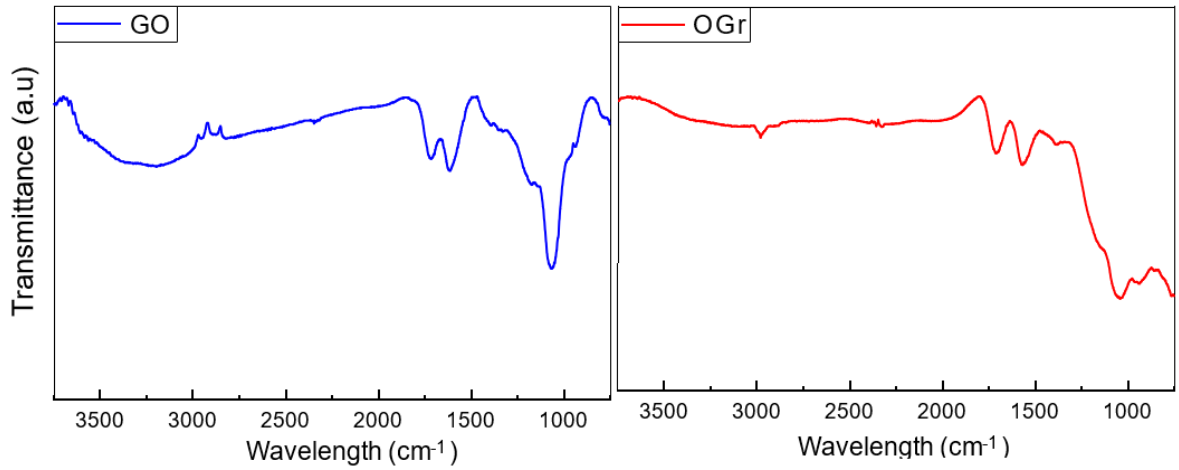


Figure 4. FTIR spectra of GO and rGO, respectively

**SEM and EDS micrograph analysis**

To determine the morphology of the samples, they were analysed in a scanning electron microscope with STEM and EDS modes. Figure 5a shows the STEM micrograph of $Mn_{0.7}$-$Zn_{0.3}Fe_2O_4$. In this case, NPs are agglomerated, this is due to their magnetic properties, since they tend to attract each other. Regarding the shape, the ferrite composition is spheroidal, therefore. Figure 5b shows a micrograph of rGO, which presents sheets stacked in random directions and confirms that they have a 2D structure. We observe that the NPFEs are grafted onto the rGO while retaining their magnetic nature, since they are agglomerated. However, it is also observed that they are dispersed in the sheets of rGO, which confirms that the nanocomposites were formed successfully.

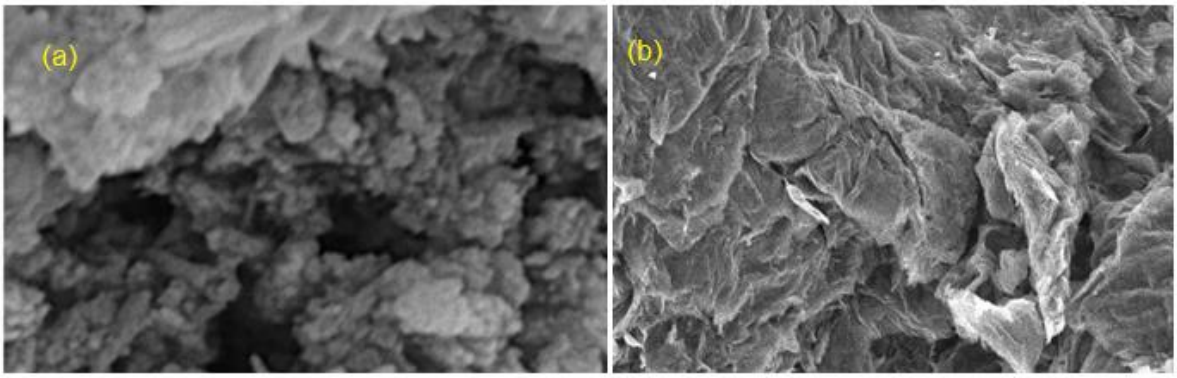


Figure 5. (a) STEM micrograph of $Mn_{0.7}$-$Zn_{0.3}Fe_2O_4$; (b) SEM micrographs of rGO

The particle size distributions (Figure 6) of the ferrite $Mn_{0.7}$-$Zn_{0.3}Fe_2O_4$, we can see that the Gaussian distribution is in the range of 4 to 10 nm. The average particle size is calculated taking into account 50 data from each sample, and the value was 9.8094 nm ($Mn_{0.7}$-$Zn_{0.3}Fe_2O_4$), with this it confirms that with the selected synthesis route nanometric-sized ferrites are obtained.

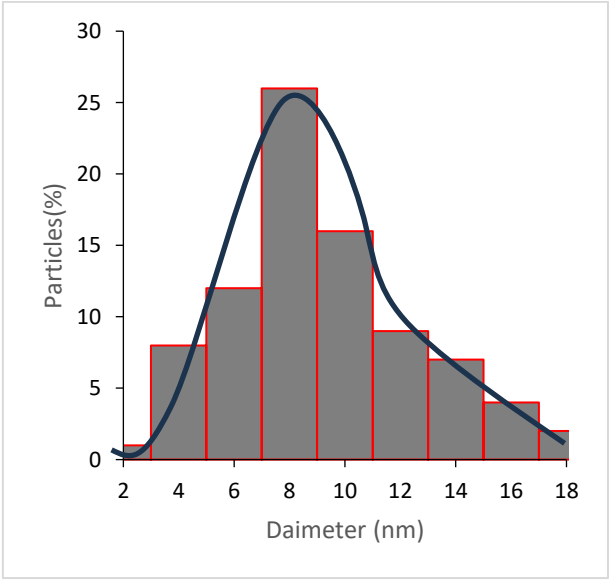


Figure 6: Particle size distribution of $Mn_{0.7}$-$Zn_{0.3}Fe_2O_4$

In Figure 7 it was observe the results of the composition of the rGO/$Mn_{0.7}$-$Zn_{0.3}Fe_2O_4$ nanocomposite through EDS analysis, obtaining 71.4% carbon, 20.3% oxygen, 5.7% iron, 1.6% manganese, 0.9% zinc, where observing and it is understandable, since a ratio of 1:0.97 of ferrite to rGO was used.

**UV-Vis Spectroscopy Analysis**

UV-Vis spectroscopy by diffuse reflectance (EDR) is used to calculate the *Eg* in powder samples as in our case. Using the Kubelka-Munk equation (equation 5) the *Eg* was calculated, this theory is valid for a particle size comparable or smaller than the wavelength of the incident light [25].

$$\frac{K}{S} = \frac{(1-R_\infty)^2}{2R_\infty} \equiv F(R_\infty) \quad (5)$$

where K is the absorption coefficient and S the scattering coefficient, $R\infty$ is the diffuse reflectance and therefore F ($R\infty$) is the diffuse reflectance function, which is what we call the Kubelka-Munk function.

Figure 8 shows the EDR spectra of $Mn_{0.7}$-$Zn_{0.3}Fe_2O_4$ sample in which the band gap energy ($Eg$) width is calculated by linear fitting; the values obtained for each sample were 1.4 eV. In the rGO/$Mn_{0.7}$-$Zn_{0.3}Fe_2O_4$ nanocomposites the $Eg$ were 1.09 eV respectively; which can be analyzed by observing Figure 9. In our research, when grafting ferrites onto the rGO sheets, the $Eg$ value decreases, which can be attributed to the generation of new energy levels above the valence band as a result of the introduction of rGO [26]. Our material confirms that it is a semiconductor, since it has an $Eg$ less than 3.0 eV and, therefore, it is a potential material as a photocatalyst.

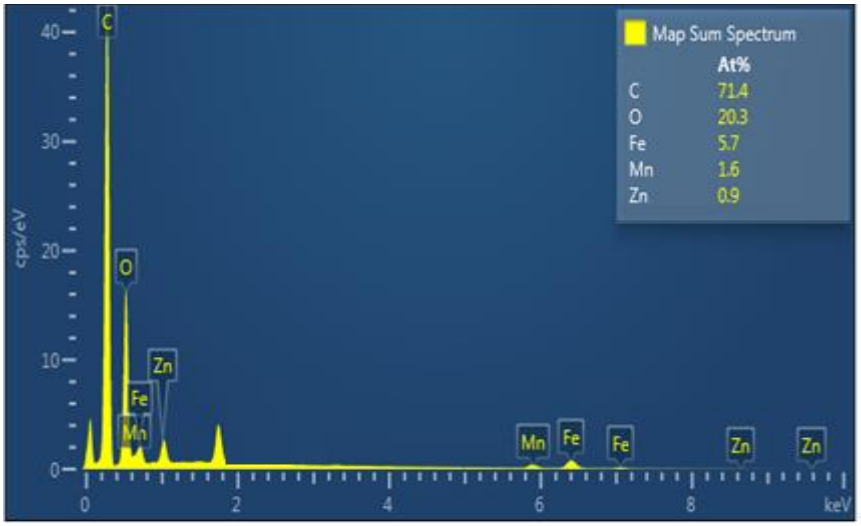


Figure 7: EDS analysis of $Mn_{0.7}$-$Zn_{0.3}Fe_2O_4$ and elemental composition

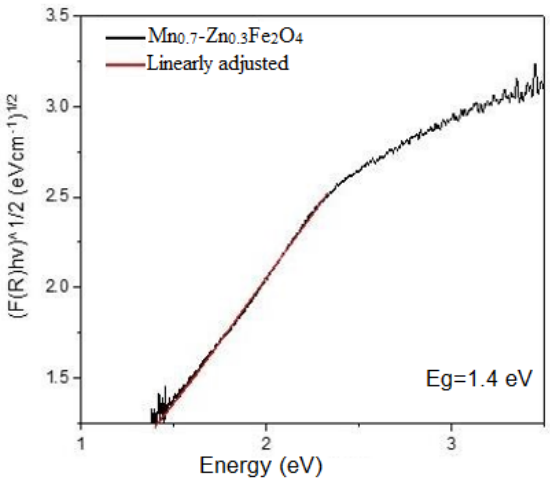


Figure 8. UV-Vis diffuse reflectance spectra of $Mn_{0.7}$-$Zn_{0.3}Fe_2O_4$ with the Kubelka-Munk function to estimate the $Eg$

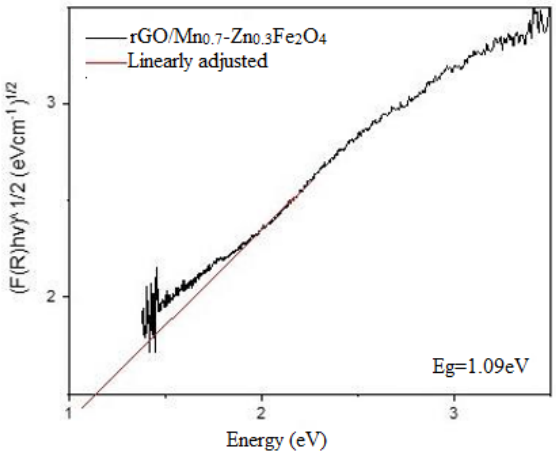


Figure 9. UV-Vis diffuse reflectance spectra of rGO/$Mn_{0.7}$-$Zn_{0.3}Fe_2O_4$ with the Kubelka-Munk function to estimate the $Eg$

**Magnetic Properties**

Magnetic properties play an important role in the application of ferrites. These properties depend on the microstructure, chemical composition, synthesis conditions and substituent ions. The variation of magnetization (M) with the applied magnetic field (H) for ferrite $Mn_{0.7}$-$Zn_{0.3}Fe_2O_4$ is presented in Figure 10 where the hysteresis curves (M-H) of sample is shown. They were carried out in a vibrating sample magnetometer at room temperature. The M-H curve shows that the ferrites behave as soft ferromagnetic materials. The ferrite presented a saturation magnetization Ms of 37.04 emu/g. This value is well below those found in the literature for Zn-Mn ferrites [27], and 66 emu/g ($ZnFe_2O_4$).

The behavior presented by ferrite can be explained by the presence of the antiferromagnetic phase α-$Fe_2O_3$, which, due to the coupling of the magnetic moment between the atoms and the adjacent ions, results in an antiparallel alignment of the magnetic moments, causing the cancellation of the magnetic dipoles. Because the ferrite presents a spinel structure and better magnetization results, it was used as a catalyst in the photo-Fenton process.

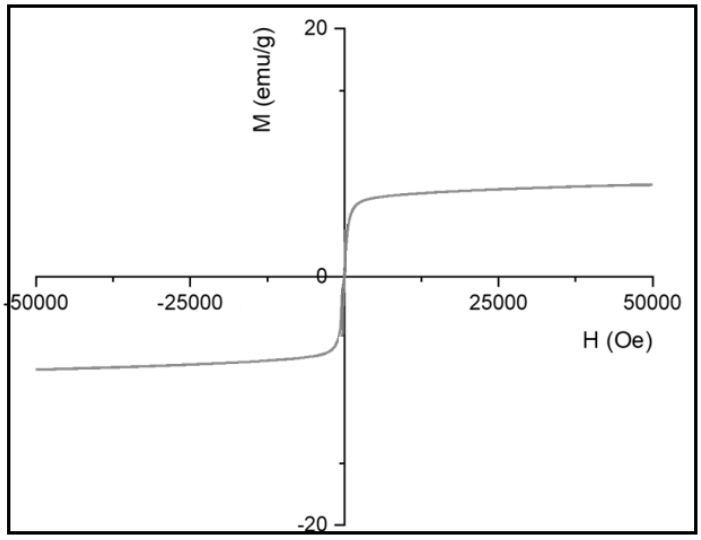


Figure 10: M-H curves of $Mn_{0.7}$-$Zn_{0.3}Fe_2O_4$ ferrite at room temperature and an applied field of 10 kOe

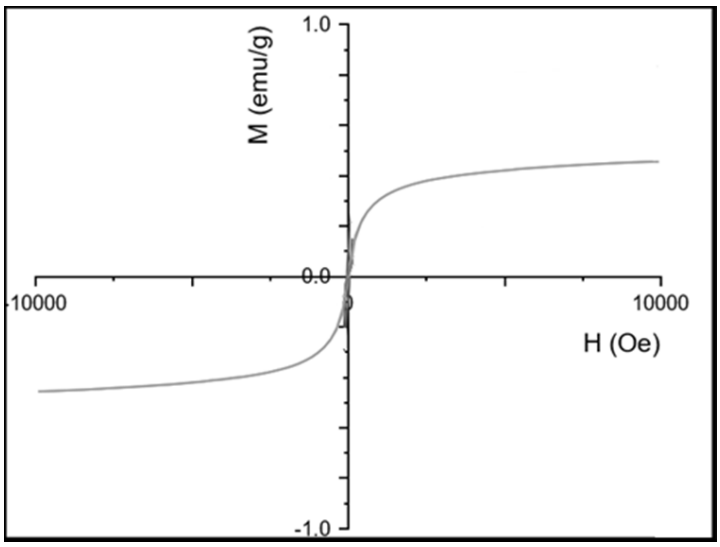


Figure 11: M-H curves of rGO/$Mn_{0.7}$-$Zn_{0.3}Fe_2O_4$ ferrite at room temperature and an applied field of 10 kOe

In Figure 11, a field of 10 kOe was applied, the graph shows that we have a mixture of ferrimagnetic and SPM behaviours. Thus, we see that the magnetization practically saturates. So, that is, as if there were a ferrimagnetic phase that saturates and a SPM that gives the non-saturation contribution. In addition, the coercivity (Hc) in the samples is considered almost null, except in the case of rGO/$Mn_{0.7}$-$Zn_{0.3}Fe_2O_4$.

Some new potentialities of multiferroic materials are being recently discovered. For BFO, photovoltaic properties have already been noted for single crystals like rGO/$Mn_{0.7}$-$Zn_{0.3}Fe_2O_4$. Results shows Mn-Zn Nanoferrites absorbing visible light, with its ferroelectric domains polarized, which consequently generate an electric current [28]. Electrical conduction occurs in the walls of the

ferroelectric domains. Hence, the photovoltaic behavior with the abrupt increase of the electric current and incidence of visible light. This behavior allows new functionalities in the areas of spintronics, optoelectronic devices, etc.

**Conclusions**

- The prepared ferrites $Mn_{0.7}$-$Zn_{0.3}Fe_2O_4$ and rGO/$Mn_{0.7}$-$Zn_{0.3}Fe_2O_4$ were successfully obtained by the CTAB-assisted sol-gel auto combustion method, since they showed the characteristic planes of the spinel-type ferrite well indexed in XRD.
- The ratio of nitrates to fuel to surfactant is crucial, as well as the choice of fuel, to synthesize a spinel-type ferrite. It is stated that the ratio 1:0.5:0.1 with urea as fuel, with a low temperature heating of 250 °C for one hour and subsequently performing a thermal treatment at 100 °C, the pure spinel phase is obtained. It is worth mentioning that crystallite sizes ranging from 7.73 nm to 21.54 nm were obtained, as well as particle sizes ranging from 7.8094 nm to 10.5165 nm.
- It is observed that pH plays a significant role in suppressing the formation of secondary phases in the solgel self-combustion synthesis route. The results indicate that a pH of 10 turns out to be the optimal condition to avoid the formation of secondary phases.
- rGO was obtained by the modified Hummer's method and subsequently by performing a chemical reduction with ascorbic acid. The XRD spectra, the SEM and the EDS confirmed that the compound was successfully carried out.
- The grafting of the NPs in the rGO sheets was carried out by the ultrasound method and the dispersion in the sheets was confirmed in SEM, although with agglomeration due to their magnetic nature.
- The materials are semiconductors since their Eg is less than 3.0 eV, and it is even very small, with value 0.97 eV, where the nanocomposites showed lower values than the ferrites. However, PL indicates that the best material for photocatalysis.

**References**

[1]. Murugesan C, Ugendar K, Okrasa L, Shen J, Chandrasekaran G. Zinc substitution effect on the structural, spectroscopic and electrical properties of nanocrystalline $MnFe_2O_4$ spinel ferrite. Ceram Int. 2021 Jan 15;47(2):1672-1685.

[2]. Nazir I, Javaid F, Baig MM, Butt MS, Gul IH. Influence of Zinc Substitution on the Structural, Dielectric, and Gas-Sensing Properties of $Mg_{1-x}Zn_xFe_2O_4$ Nanoparticles. ACS Omega. 2023 Sep 14;8(38):34760-34767.

[3]. Anegbe, B., Ifijen, I.H., Maliki, M. *et al.* Graphene oxide synthesis and applications in emerging contaminant removal: a comprehensive review. *Environ Sci Eur* **36**, 15 (2024). https://doi.org/10.1186/s12302-023-00814-4

[4]. Viprya, P., Kumar, D., & Kowshik, S. (2023). Study of Different Properties of Graphene Oxide (GO) and Reduced Graphene Oxide (rGO). *Engineering Proceedings*, *59*(1), 84. https://doi.org/10.3390/engproc2023059084

[5]. Sindi AM. Applications of graphene oxide and reduced graphene oxide in advanced dental materials and therapies. J Taibah Univ Med Sci. 2024 Feb 18;19(2):403-421. doi: 10.1016/j.jtumed.2024.02.002.

[6]. Alam, S. , Sharma, N. and Kumar, L. (2017) Synthesis of Graphene Oxide (GO) by Modified Hummers Method and Its Thermal Reduction to Obtain Reduced Graphene Oxide (rGO)*. *Graphene*, **6**, 1-18. doi: 10.4236/graphene.2017.61001.

[7]. Kanika Sharma, Nupur Aggarwal, Naveen Kumar, Anjana Sharma, A review paper: Synthesis techniques and advance application of Mn-Zn nano-ferrites, Materials Today: Proceedings, 2023,https://doi.org/10.1016/j.matpr.2022.12.088.

[8]. Gopalan, Veena & Al-Omari, Imaddin & Malini, K A & Joy, Pattayil & Kumar, Sakthi & Yoshida, Yasuhiko & Anantharamaniyer, Maliemadom. (2009). Impact of Zinc Substitution on the Structural and Magnetic Properties of Chemically Derived Nanosized Manganese Zinc Mixed Ferrites. Journal of Magnetism and Magnetic Materials - J MAGN MAGN MATER. 321. 1092-1099. 10.1016/j.jmmm.2008.10.031.

[9]. Hessien, M.A., Khattab, R.M. & Sadek, H.E.H. Synthesis and Characterization of ZnO, $Mn_3O_4$, and $ZnMn_2O_4$ Spinel by New Chelation-Precipitation Method: Magnetic and Antimicrobial Properties. *J Inorg Organomet Polym* (2024). https://doi.org/10.1007/s10904-024-03489-3

[10]. Abdel-Fattah Omran, Mohamed. (2014). Polyaniline–Zn0.2Mn0.8 Fe2O4 ferrite core–shell composite: Preparation, characterization and properties. Journal of Alloys and Compounds. 608. 283-291. 10.1016/j.jallcom.2014.04.130.

[11]. Othman, Ibraheem & Mostafa, Ahmed. (2015). Photocatalytic reduction of chromate oxyanions on MMnFe2O4 (M=Zn, Cd) nanoparticles. Materials Science in Semiconductor Processing. 33. 10.1016/j.mssp.2015.01.030.

[12]. Anwar, Armin & Akter, Ayesha & Khan, Mohammed. (2021). Effect of Mn2+ substitution on structural, morphological, and electrical properties of Ba0.4Ca0.4Sr0.2MnxTi1−xO3 perovskites. Conference: 6th Conference of Bangladesh Crystallographic Association (BCA 2021) Dhaka, Bangladesh

[13]. Arguello Cruz, E., Ducos, P., Gao, Z., Johnson, A. T. C., & Niebieskikwiat, D. (2023). Exchange Coupling Effects on the Magnetotransport Properties of Ni-Nanoparticle-Decorated Graphene. *Nanomaterials*, *13*(12), 1861. https://doi.org/10.3390/nano1312186.

[14]. Medina, A., Casado-Carmona, F. A., López-Lorente, Á. I., & Cárdenas, S. (2020). Magnetic Graphene Oxide Composite for the Microextraction and Determination of Benzophenones in Water Samples. *Nanomaterials*, *10*(1), 168. https://doi.org/10.3390/nano10010168

[15]. Alam, S. , Sharma, N. and Kumar, L. (2017) Synthesis of Graphene Oxide (GO) by Modified Hummers Method and Its Thermal Reduction to Obtain Reduced Graphene Oxide (rGO)*. *Graphene*, **6**, 1-18. doi: 10.4236/graphene.2017.61001.

[16]. Vozniuk, Olena & Bazzo, Cristian & Albonetti, Stefania & Tanchoux, Nathalie & Bosselet, Françoise & Millet, J.M.M. & Di Renzo, Francesco & Cavani, Fabrizio. (2017). Structural Changes of Binary/Ternary Spinel Oxides During Ethanol Anaerobic Decomposition. ChemCatChem. 9. 10.1002/cctc.201601605.

[17]. Stewart, S. J., Figueroa, S. J. A., Ramallo López, J. M., Marchetti, S. G., Bengoa, J. F., Prado, R. J., Requejo, F. G. (2007) Cationic exchange in nanosizedZnFe2O4spinel revealed by experimental and simulated near-edge absorption structure. Physical Review B, 75 (7)

[18]. Holzwarth U, Gibson N. The Scherrer equation versus the 'Debye-Scherrer equation'. Nat Nanotechnol. 2011 Aug 28;6(9):534. doi: 10.1038/nnano.2011.145.

[19]. Fan, Z., Wang, K., Wei, T., Yan, J., Song, L., & Shao, B. (2010). An environmentally friendly and efficient route for the reduction of graphene oxide by aluminum powder. Carbon, 48(5), 1686-1689.

[20]. Lin, J., Yang, X., Su, K., Yang, F., He, Y., & Lin, Q. (2023). Effects of Nonmagnetic $Zn^{2+}$ Ion and RE Ion Substitution on the Magnetic Properties of Functional Nanomaterials $Co_{1-y}Zn_yRE_xFe_{2-x}O_4$ (RE = La, Sm, Gd) by Sol–Gel. *Molecules*, *28*(17), 6280. https://doi.org/10.3390/molecules28176280

[21]. Stobinski, L., Lesiak, B., Malolepszy, A., Mazurkiewicz, M., Mierzwa, B., Zemek, J., Bieloshapka, I. (2014). Graphene oxide and reduced graphene oxide studied by the XRD, TEM and electron spectroscopy methods. Journal of Electron Spectroscopy and Related Phenomena, 195, 145-154

[22]. Ahmed, A., Usman, M., Wang, S., Yu, B., Shen, Y., & Cong, H. (2021). Facile synthesis of Zr4+ substituted Mn0.2Co0.8Fe2−xO4 nanoparticles and their composites with reduced graphene oxide for enhanced photocatalytic performance under visible light irradiation. Synthetic Metals, 277, 116766

[23]. Jagiełło, J., Chlanda, A., Baran, M., Gwiazda, M., & Lipińska, L. (2020). Synthesis and Characterization of Graphene Oxide and Reduced Graphene Oxide Composites with Inorganic Nanoparticles for Biomedical Applications. *Nanomaterials*, *10*(9), 1846. https://doi.org/10.3390/nano10091846.

[24]. Ghann, W. E., Kang, H., Uddin, J., Chowdhury, F. A., Khondaker, S. I., Moniruzzaman, M., Kabir, M. H., & Rahman, M. M. (2019). Synthesis and Characterization of Reduced Graphene Oxide and Their Application in Dye-Sensitized Solar Cells. *ChemEngineering*, *3*(1), 7. https://doi.org/10.3390/chemengineering3010007.

[25]. Rodríguez-Mas, F., Ferrer, J. C., Alonso, J. L., Valiente, D., & Fernández de Ávila, S. (2020). A Comparative Study of Theoretical Methods to Estimate Semiconductor Nanoparticles' Size. Crystals, 10(3), 226. https://doi.org/10.3390/cryst10030226

[26]. Li, Z., Chen, H., & Liu, W. (2018). Full-Spectrum Photocatalytic Activity of ZnO/CuO/$ZnFe_2O_4$ Nanocomposite as a PhotoFenton-Like Catalyst. *Catalysts*, *8*(11), 557. https://doi.org/10.3390/catal8110557

[27]. V. J. Silva, A. P. A Diniz, P. T. A. Santos, D. A. Vieira, A. C. F. M. Costa, D. R. Cornejo, L. Gama, Revista Eletrônica Mater. Proc. 1 (2006) 09.

[28]. Spaldin, N.A., Cheong, S.W. and Ramesh, R. (2010) Multiferroics: Past, Present, and Future. Physics Today, 63, 38.https://doi.org/10.1063/1.3502547